The Ll.LtrB intron from *Lactococcus lactis* excises as circles in vivo: insights into the group II intron circularization pathway

CAROLINE MONAT, CECILIA QUIROGA, FELIX LAROCHE-JOHNSTON, and BENOIT COUSINEAU

Department of Microbiology and Immunology, Microbiome and Disease Tolerance Centre (MDTC), McGill University, Montréal, Québec, Canada H3A 2B4

ABSTRACT

Group II introns are large ribozymes that require the assistance of intron-encoded or free-standing maturases to splice from their pre-mRNAs in vivo. They mainly splice through the classical branching pathway, being released as RNA lariats. However, group II introns can also splice through secondary pathways like hydrolysis and circularization leading to the release of linear and circular introns, respectively. Here, we assessed in vivo splicing of various constructs of the Ll.LtrB group II intron from the Gram-positive bacterium *Lactococcus lactis*. The study of excised intron junctions revealed, in addition to branched intron lariats, the presence of perfect end-to-end intron circles and alternatively circularized introns. Removal of the branch point A residue prevented Ll.LtrB excision through the branching pathway but did not hinder intron circle formation. Complete intron RNA circles were found associated with the intron-encoded protein LtrA forming nevertheless inactive RNPs. Traces of double-stranded head-to-tail intron DNA junctions were also detected in *L. lactis* RNA and nucleic acid extracts. Some intron circles and alternatively circularized introns harbored variable number of non-encoded nucleotides at their splice junction. The presence of mRNA fragments at the splice junction of some intron RNA circles provides insights into the group II intron circularization pathway in bacteria.

Keywords: group II intron; intron circle; alternative splicing; circularization pathway; head-to-tail intron DNA junction

INTRODUCTION

Group II introns were initially found interrupting mitochondrial and chloroplastic genes of higher plants, and mitochondrial genes of lower eukaryotes. More recently, group II introns were discovered in both Gram-negative and Gram-positive bacteria; about one-quarter of all sequenced bacterial genomes harboring one to a few copies. In contrast, group II introns are relatively infrequent in archaea and absent from the nuclear genome of eukaryotes (Ferat and Michel 1993; Lambowitz and Zimmerly 2004, 2011). Despite a lack of similitude at the primary sequence level, the secondary structure of group II introns is well conserved, consisting of six domains (DI–DVI) that radiate from a central wheel (Fedorova and Zingler 2007). Some group II introns harbor a multifunctional open reading frame (ORF) encoded in the loop region of domain IV. A number of these ORF-containing introns were studied as model systems and shown to be retromobile genetic elements. Mobile group II introns invade new DNA sites using an RNA intermediate and target either identical or similar sequences by retrohoming or retrotransposition respectively (Lambowitz and Zimmerly 2004, 2011). From an evolutionary standpoint, group II introns are believed to be at the origin of more than half of the human genome because they are considered as the ancestors of the highly abundant non-LTR retrotransposons and spliceosome-dependent nuclear introns. Small nuclear RNAs (snRNAs), that are part of the spliceosome, are also believed to have originated from fragments of an ancestral group II intron (Cech 1986; Sharp 1991; Michel and Ferat 1995; Lambowitz and Zimmerly 2004, 2011).

Group II introns need the assistance of proteins called maturases to self-splice from pre-mRNAs in vivo. However, these large ribozymes can splice in the absence of their splicing factor in vitro under high salt conditions. The most studied and main group II intron splicing pathway is the branching pathway (Fig. 1A; Fedorova and Zingler 2007). Following transcription of the interrupted gene, the first nucleophilic attack at the exon 1–intron junction is initiated by the 2′-OH residue of a bulged adenosine (A), called the branch point, located near the 3′ end of the intron (Fig. 1A, step 1). This transesterification reaction connects the 5′ end of the intron to the branch point and releases exon 1 that remains associated to the intron through base-pairing

Corresponding author: benoit.cousineau@mcgill.ca

Article published online ahead of print. Article and publication date are at http://www.rnajournal.org/cgi/doi/10.1261/rna.046367.114.

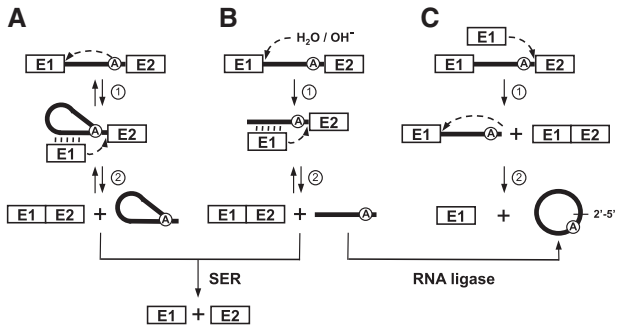

FIGURE 1. Group II intron splicing pathways. (*A*) Branching pathway. Following transcription of the interrupted gene, the 2′-OH residue of the branch-point nucleotide (A) performs the first nucleophilic attack at the exon 1–intron junction (step 1). This transesterification reaction connects the 5′ end of the intron to the branch point and releases exon 1 that remains associated to the intron through base-pairing interactions (EBS–IBS interactions, vertical lines). The liberated 3′-OH at the end of exon 1 then initiates a second nucleophilic attack at the intron–exon 2 junction (step 2), ligating the two exons and releasing the intron as a lariat. (*B*) Hydrolytic pathway. A water molecule or a hydroxyl ion initiates the first nucleophilic attack at the exon 1–intron junction (step 1). The second nucleophilic attack at the intron–exon 2 junction is initiated by the liberated 3′-OH at the end of exon 1 (step 2) which ligates the two exons and releases a linear intron. (*C*) Circularization pathway. The first nucleophilic attack at the intron–exon 2 junction is initiated by the 3′-OH of a free exon 1 (step 1). The 2′-OH of the last intron residue is thought to initiate the second nucleophilic reaction at the exon 1–intron junction (step 2) resulting in intron circularization and the release of free exon 1. A potential source of free exon 1 is the spliced exon reopening (SER) reaction where both excised lariats and linear introns can recognize and hydrolyze ligated exons at the splice junction. An alternative pathway for intron circle formation is the potential circularization of an excised linear intron by a host-encoded RNA ligase.

interactions. The liberated 3′-OH of exon 1 then initiates the second transesterification reaction at the intron–exon 2 junction, ligating the two flanking exons and releasing the intron RNA in the form of a lariat (Fig. 1A, step 2).

Group II introns can also splice through secondary splicing pathways like the hydrolytic (Fig. 1B) and circularization (Fig. 1C) pathways that are not as well characterized as branching, especially in vivo (Fedorova and Zingler 2007; Pyle 2010). During hydrolysis the first nucleophilic attack is induced by a water molecule or a hydroxyl ion (Fig. 1B, step 1), while the second step proceeds as in the branching pathway (Fig. 1B, step 2). The hydrolytic pathway thus releases linear introns instead of lariats. In the proposed circularization pathway (Murray et al. 2001; Fedorova and Zingler 2007), the first step is initiated by the 3′-OH of a free exon 1 attacking the phosphodiester bond at the intron–exon 2 junction (Fig. 1C, step 1). The second transesterification reaction is initiated by the 2′-OH of the last nucleotide of the intron leading to the release of the intron as a closed circle and free exon 1 (Fig. 1C, step 2). A potential source of free exon 1, needed for the initiation of the circularization pathway, may come from the spliced exon reopening reaction (SER) (Jarrell et al. 1988). SER consists of the hydrolysis of ligated exons by reverse splicing of a lariat or a linear intron precisely at the splice junction between both exons (Fig. 1, SER). An alternative pathway for intron circle formation would involve the circularization of a released linear intron by a host-encoded RNA ligase (Fig. 1, RNA ligase). However, given the complex tridimensional structure of group II introns, it is unlikely that an RNA ligase would be able to bring the 5′ and 3′ ends in close proximity for ligation. Intron RNA circles were previously observed in vitro (Murray et al. 2001; Nagy et al. 2013) and in vivo (Li-Pook-Than and Bonen 2006; Molina-Sánchez et al. 2006, 2011; Dalby and Bonen 2013) but the circularization pathway was not addressed. Interestingly, the presence of intron RNA circles in vivo can be accompanied by traces of head-to-tail intron DNA junctions (Osiewacz and Esser 1984; Schmidt et al. 1994; Begel et al. 1999; Murray et al. 2001; Molina-Sánchez et al. 2006; Federova and Zingler 2007). The nature, the origin and the function of these intron DNA junctions where the 5′ and 3′ end of the intron are precisely joined is still unclear. In addition, splicing products involving either 5′ or 3′ alternative splice sites were recently detected for different group II introns in vitro (Costa et al. 2006a,b; Toor et al. 2006; Stabell et al. 2007; Chee and Takami 2011). However, very few examples of in vivo alternative splicing events were reported (Robart et al. 2004; Tourasse et al. 2005; McNeil et al. 2014).

Here, we assessed Ll.LtrB splicing in vivo by studying the splice junction of released introns by RT-PCR. Our data revealed the presence of intron lariats, perfect end-to-end intron circles and alternatively circularized intron products for all Ll.LtrB variants studied, albeit at different ratios. Removal of the branch point A residue only prevented Ll.LtrB excision through the branching pathway. Complete intron RNA circles were detected and found associated with LtrA forming ribonucleoprotein particles (RNPs) in vivo. However, no mobility products of Ll.LtrB-ΔA where detected suggesting that RNPs containing circular introns are not active and cannot invade new sites. Traces of head-to-tail intron DNA junctions were also detected from *Lactococcus lactis* RNA and nucleic acid extracts and shown to be double-stranded. We also discovered that the splice junction of some circular introns harbor extra non-encoded nucleotides. The presence of mRNA fragments at the junction of some intron RNA circles provides experimental support to the proposed intron circularization splicing pathway. This study demonstrates that Ll.LtrB excises as both lariats and circles in vivo while shedding light on the mechanism of group II intron circularization in bacteria.

RESULTS

Ll.LtrB excises as lariats and circles in vivo

Splicing of different Ll.LtrB constructs was assesed by amplifying the splice junction of released introns from *L. lactis* total RNA extracts (Fig. 2A; Belhocine et al. 2007, 2008). Functional splicing assays previously showed that Ll.LtrB

encoding a maturase mutant of LtrA (Ll.LtrB-LtrAMat$^-$) or missing most of the LtrA coding sequence (Ll.LtrB-ΔLtrA) splice, respectively, 25- and 380-fold less efficiently than Ll.LtrB-WT (Belhocine et al. 2007). However, providing LtrA in trans from a second plasmid (Ll.LtrB-ΔLtrA+LtrA) completely rescued the splicing of Ll.LtrB-ΔLtrA to WT level (Belhocine et al. 2008).

The expected RT-PCR band of 287 bp, corresponding to released intron lariats, was present for all constructs along with additional smaller bands (Fig. 2B). Products of the amplification reactions were cloned and sequenced revealing that only Ll.LtrB-WT and Ll.LtrB-ΔLtrA+LtrA produce significant amounts of intron lariats (Fig. 2C; Supplemental Table S1). As previously observed, the branched adenosine was misread by the RT enzyme during cDNA synthesis; most of the time an A was incorporated instead of a T (Supplemental Table S1; Vogel et al. 1997, 2002; Carrillo et al. 2001; Li-Pook-Than and Bonen 2006; Molina-Sánchez et al. 2006; Dalby and Bonen 2013).

We also detected for all constructs the presence of Ll.LtrB RNA circles where the 5′ and 3′ ends are perfectly joined (Fig. 2C; Supplemental Table S1). Intron RNA circles consisted of the great majority of the clones for Ll.LtrB-ΔA but they contained an extra C at the junction. Similarly, the majority of the Ll.LtrB-LtrAMat$^-$ RNA circles harbored an extra C residue at the splice junction. On the other hand, the Ll.LtrB-WT RNA circles were all perfect while only 3 of the 18 Ll.LtrB-ΔLtrA+LtrA RNA circles harbored extra non-encoded nucleotides at their splice junction (1 nt, 27 nt, or 31 nt) (Supplemental Table S1).

All intron constructs lead to some level of alternative circularization including Ll.LtrB-WT and Ll.LtrB-ΔLtrA+LtrA while alternatively circularized products corresponded to the majority of the clones for the splicing deficient introns Ll.LtrB-LtrAMat$^-$ and Ll.LtrB-ΔLtrA (Fig. 2C). Some products of alternative circularization also harbored small streches of additional non-encoded nucleotides at the splice juntion (3–7 nt) (Supplemental Table S1).

Overall, our results show the presence of intron lariats, perfect end-to-end intron circles and alternatively circularized introns in total RNA extracts of *L. lactis* expressing all the Ll.LtrB constructs studied except Ll.LtrB-ΔA for which no lariats were detected. These data demonstrate that Ll.LtrB does not exclusively splice through the branching pathway in vivo and that the 5′ and 3′ splice junctions are not always recognized accurately during splicing.

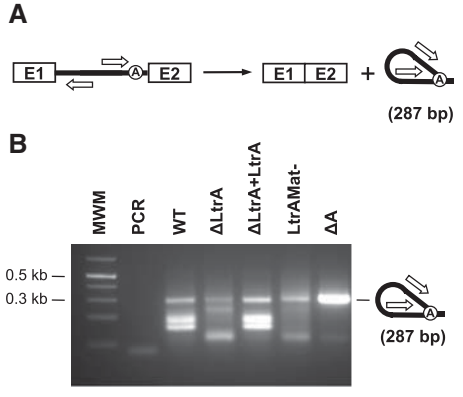

C

	Lariats	Circles	Alt. Cir.
Ll.LtrB-WT	30	11	12
Ll.LtrB-ΔLtrA	1	2	19*
Ll.LtrB-ΔLtrA+LtrA	18	18*	14
Ll.LtrB-LtrAMat-	1	9*	42*
Ll.LtrB-ΔA	0	31*	2

FIGURE 2. RT-PCR amplification of excised intron junctions. (*A*) Schematic of the Ll.LtrB splicing pathway (branching). Position of the primers used to amplify the intron splice junction is depicted (open arrows, 287 bp). (*B*) RT-PCR amplifications performed on total RNA extracts from *L. lactis* (NZ9800Δ*ltrB*) harboring different Ll.LtrB constructs expressed under the control of the P_{23} constitutive promoter. (*C*) RT-PCR amplicons of excised introns (*B*) were phosphorylated and cloned in pBS (SmaI). Their sequences (Supplemental Table S1) correspond to lariats, circles, or alternatively circularized products (Alt. Cir.). Some of the intron junctions denoted by an asterisk have additional non-encoded nucleotides at the splice junction (Supplemental Table S1).

Complete Ll.LtrB RNA circles are associated to LtrA in vivo

To further characterize released intron RNAs in vivo, we used an RT-PCR assay generating smaller amplicons of 138 bp (lariats) or 144 bp (circles). Both intron forms were detected regardless of the *L. lactis* growth phase confirming that Ll.LtrB-WT excises as both lariats and circles in vivo (Fig. 3A). Compared with intron lariats, we noticed a slight accumulation of the Ll.LtrB RNA circles with time (Fig. 3A). In accordance with our previous RT-PCR results (Fig. 2C), very little lariat was detectable for Ll.LtrB-ΔLtrA and Ll.LtrB-LtrAMat$^-$ while Ll.LtrB-ΔA excised exclusively as circles in exponentially growing *L. lactis* (7 h time point) (Fig. 3B).

We next assessed if the intron RNA circles are associated with LtrA forming RNPs in vivo. LtrA was immunoprecipitated (IP) from crude cell extracts. IP reactions were treated with DNase I and proteinase K before the intron splice junction was amplified by RT-PCR. Lariats and circles were detected for both Ll.LtrB-WT and Ll.LtrB-ΔLtrA+LtrA while only circles were detected for Ll.LtrB-ΔA (Fig. 3C). Longer gel exposures revealed bands corresponding to both intron circles and lariats for Ll.LtrB-LtrAMat$^-$ (data not shown). Another RT-PCR assay was then designed to specifically amplify complete intron RNA circles from LtrA IP reactions. One of the primers was complementary to the circular intron splice junction (D0), annealing with 11 nt on each side, while the other primer was only 5 nt away and complementary to the opposite strand (D1) (Fig. 3D). Bands of 2.5 kb corresponding to complete intron RNA circles were obtained for Ll.LtrB-WT, Ll.LtrB-LtrAMat$^-$, and Ll.LtrB-ΔA. As expected, the Ll.LtrB-ΔLtrA+LtrA circles were significantly smaller (0.8

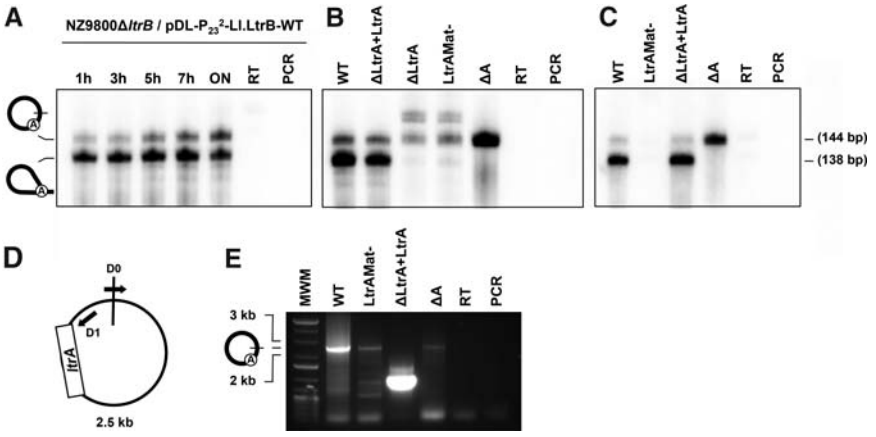

FIGURE 3. Ll.LtrB RNA circles form RNPs in vivo. A primer pair was designed to amplify both the lariat (138 bp) and the circular intron junctions (144 bp) from the same RT-PCR reaction (*A–C*). An alternative RT-PCR strategy was used to amplify complete intron RNA circles (*D–E*). (*A*) RT-PCR performed on total RNA extracted from aliquots of a bacterial culture (NZ9800Δ*ltrB*/pDL-P_{23}^{2}-Ll.LtrB-WT) taken at different time points. (*B*) RT-PCR performed on total RNA extracted from aliquots of bacterial cultures (7 h) expressing different Ll.LtrB variants. The slower migrating bands amplified from the Ll.LtrB-ΔLtrA and Ll.LtrB-LtrAMat^{-} RNA extracts correspond to non-specifc amplifications. (*C*) RT-PCR performed on intron RNA recovered by immunoprecipitation of the LtrA protein from total cell lysates. (*D*) Schematic of intron RNA circles showing the position of the two primers used to amplify complete intron RNA circles by RT-PCR. One primer is complementary to the perfect intron circle junction base-pairing with 11 nt on each sides (D0) while the other primer is only 5 nt away (D1). (*E*) RT-PCR of complete intron RNA circles using intron RNA isolated by immunoprecipitation of the LtrA protein.

kb) owing to the absence of the LtrA ORF from DIV (1.7 kb) (Fig. 3E). These amplicons were sequenced confirming the presence of Ll.LtrB RNPs harboring complete intron RNA circles in vivo.

Mobility of the Ll.LtrB-ΔA intron, which almost exclusively splices as circles, was assessed using a two-plasmid mobility assay (Cousineau et al. 1998, 2000). Ll.LtrB-ΔA and a variant marked with the Retrohoming Indicator Gene (RIG, Ichiyanagi et al. 2002) (Ll.LtrB-ΔA-RIG), which confers kanamycin resistance upon reinsertion, were both tested. Both introns were independently overexpressed from an intron donor plasmid in the presence of a co-transformed intron recipient plasmid, harboring the intron homing site. Even though both intron variants were shown to produce RNA circles in vivo, no trace of mobility products were detected for either suggesting that RNPs composed of LtrA and the Ll.LtrB-ΔA circular introns are not active for retrohoming in *L. lactis*.

These data show the presence of full-length RNA circles for all the Ll.LtrB constructs studied. They also demonstrate that full-length intron RNA circles can be found associated to LtrA in vivo but are most likely not mobile.

Detection of double-stranded head-to-tail intron DNA junctions in *L. lactis*

Additional RT-PCR reactions were performed on *L. lactis* total RNA extracts either untreated, treated with RNase A, or treated with DNase I (Fig. 4). Intense bands corresponding to released intron lariats (138 bp) (Ll.LtrB-WT, Ll.LtrB-ΔLtrA+LtrA) and circles (144 bp) (Ll.LtrB-ΔA) only appeared when reverse transcription was performed before PCR, confirming that they correspond to RNA molecules (Fig. 4A). PCR bands of 144 bp were detected for all constructs when the reverse transcription step was omitted suggesting the presence of head-to-tail intron DNA junctions where the 5′ and 3′ ends of the intron are joined (Fig. 4A). When total RNA extracts were pretreated with RNase A, the intense bands corresponding to RNA lariats (Ll.LtrB-WT, Ll.LtrB-ΔLtrA+LtrA) and circles (Ll.LtrB-ΔA) disappeared, whereas the bands likely corresponding to head-to-tail intron DNA junctions were still present regardless of whether the reverse transcription step was performed (Fig. 4B). In addition, these amplicons of 144 bp disappeared when the RNA extracts were pretreated with DNase I and not reverse transcribed before PCR (Fig. 4C) confirming the presence of head-to-tail intron DNA junctions for all constructs. However, the presence of RT-specifc bands of 138 and 144 bp from RNA extracts pretreated with DNase I corroborates the presence of intron RNA lariats (Ll.LtrB-WT, Ll.LtrB-ΔLtrA+LtrA) and intron RNA circles (Ll.LtrB-WT, Ll.LtrB-ΔLtrA+LtrA and Ll.LtrB-ΔA) (Fig. 4C).

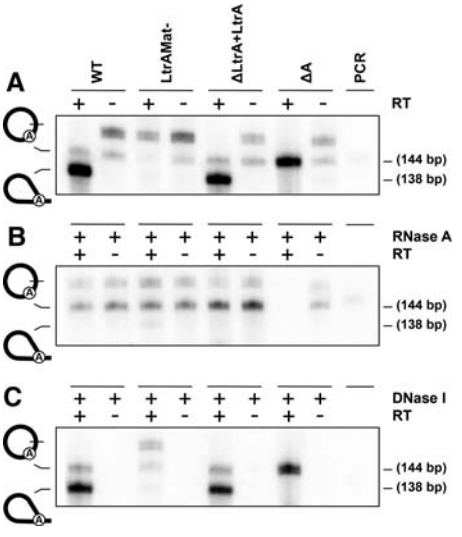

FIGURE 4. Detection of head-to-tail intron DNA junctions. Total RNA extracts from *L. lactis* carrying various Ll.LtrB constructs were either untreated (*A*), treated with RNase A (*B*), or treated with DNase I (*C*) prior to RT-PCR amplification of the released intron junction (intron lariat, 138 bp; intron circle, 144 bp).

Next, we PCR amplified and cloned the predicted head-to-tail intron DNA junctions from total nucleic acid extract of Ll.LtrB-WT treated with RNase A (Fig. 4B). The majority of the clones (23/26) corresponded to a perfect 5′–3′ intron junction while two clones harbored an extra G at the splice junction and a T instead of A at the branch point position. In addition, one clone was missing 27 nt at the junction: 2 nt from the 5′ end and 25 nt from the 3′ end of the intron (Supplemental Fig. S1A). To assess if the head-to-tail intron DNA junctions detected are double-stranded, we digested the RNase A treated nucleic acid extract with BsiWI before PCR. This restriction enzyme has a recognition site near the 3′ end of the intron and strictly cuts double-stranded DNA. In order to include the BsiWI recognition site within the amplified spliced intron junction we used a primer that is 31 nt further upstream at the 3′ end of the intron. In sharp contrast, BsiWI treatment inhibited the amplification of head-to-tail intron DNA junctions; only one clone (1/13) corresponded to a perfect 5′–3′ intron junction but harbored a G instead of an A at the branch point. All the other clones were missing some nucleotides and showed none or very little homology at the junction (Supplemental Fig. S1B).

Using various experimental approaches including DNA circle recovery with Tn5 transposons harboring an origin of replication (R6Kγori) and amplification of full intron DNA circles by PCR, we were not able to isolate or detect full-length intron DNA circles from *L. lactis* nucleic acid extracts.

Taken together, our data show the presence of head-to-tail DNA junctions for all the Ll.LtrB constructs studied and suggest that these DNA junctions are most likely double-stranded.

DISCUSSION

In this study, we examined the intron splicing products generated in vivo by variants of the Ll.LtrB group II intron from *L. lactis*. Overall, the analysis of released intron junctions revealed that in addition to intron lariats, perfect end-to-end intron RNA circles and alternatively circularized intron products are also present for all constructs. Our data thus reveal that Ll.LtrB does not splice exclusively through to the main classical branching pathway in vivo. We cannot precisely assess the relative abundance between intron lariats and circles because the RT enzyme is not as processive going through the 2′–5′ link found at the branch point of lariats during the RT-PCR assays. However, our data demonstrate that a significant proportion of these introns excise as circles in *L. lactis*.

Circularized intron products, where the 5′ and/or 3′ splice sites were not properly recognized, were also found for all the Ll.LtrB variants studied albeit at different levels showing that even the wild-type intron uses alternative splice sites in vivo (Fig. 2C; Supplemental Table S1). Some of these aberrantly circularized introns harbored small stretches of non-encoded nucleotides (3–7 nt) at their splice junction (Supplemental Table S1). The detection of such a variety of alternatively circularized intron products may be due to the fact that excised circular introns should be protected from exonucleases because they do not have free 5′ and 3′ ends. This could increase their stability in vivo potentially contributing to their accumulation.

It was previously reported that when intron RNA circles are found, intron DNA circles or at least head-to-tail intron DNA junctions could also be detected (Osiewacz and Esser 1984; Schmidt et al. 1994; Begel et al. 1999; Murray et al. 2001; Molina-Sánchez et al. 2006; Federova and Zingler 2007). However, the origin, the nature, and the significance of these head-to-tail intron DNA junctions are still unclear. Similarly, we detected by RT-PCR the presence of head-to-tail intron DNA junctions from total RNA of all Ll.LtrB constructs studied (Fig. 4). The head-to-tail intron DNA junctions were PCR amplified and cloned from nucleic acid extracts of Ll.LtrB-WT (Supplemental Fig. S1A). These head-to-tail intron DNA junctions were no longer detectable when total RNA extracts were treated with DNase I (Fig. 4) or when the nucleic acid extracts were incubated with BsiWI before PCR (Supplemental Fig. S1B). In addition, no significant stretches of homology could be detected on both sides of the cloned intron DNA junctions. Taken together, these data suggest that the head-to-tail DNA junctions of Ll.LtrB are double-stranded and generated by a pathway not requiring intron mobility and no significant sequence homology.

As previously observed (Li-Pook-Than and Bonen 2006; Molina-Sánchez et al. 2006, 2011; Dalby and Bonen 2013), we detected some perfect intron RNA circles harboring extra nucleotides at the splice junction (Supplemental Table S1). The majority of the intron RNA circles for Ll.LtrB-LtrAMat$^-$ (8/9) and Ll.LtrB-ΔA (30/31) harbored an extra C at the junction. Importantly, two Ll.LtrB-ΔLtrA+LtrA intron RNA circles were found harboring long streches of 27 and 31 non-encoded nucleotides (Supplemental Table S1). These sequences were identified as perfect matches to mRNA fragments encoded either in the *L. lactis* genome (ribosomal protein L21 gene, 31 nt) or on the pLE resident plasmid (chloramphenicol resistance gene, 27 nt). The presence of these long mRNA segments at the splice junction of Ll.LtrB-ΔLtrA+LtrA circles suggests that fragments of cellular RNAs can be incorporated at the splice junction during intron circularization.

Two variations of the circularization pathway were previously proposed to explain the presence of non-encoded nucleotides at the splice junction of group II intron RNA circles (Fig. 5; Li-Pook-Than and Bonen 2006). In the first pathway (Fig. 5A), following the release of introns through hydrolysis (steps 1 and 2), non-encoded nucleotides would be incorporated at the 3′ end of linear introns before or during circularization by an unknown mechanism (step 3). In the alternative pathway (Fig. 5B), the 3′-OH residue of an exogenous RNA molecule would attack the intron 5′ splice site displacing exon 1 (step 1). Similarly to the circularization

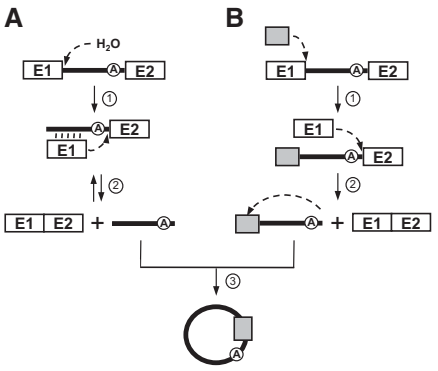

FIGURE 5. Models for incorporation of non-encoded nucleotides in intron RNA circles. Non-encoded nucleotides (gray box) may be incorporated during splicing using variations of the hydrolytic (*A*) (Fig. 1B) or circularization pathway (*B*) (Fig. 1C). (*A*) Non-encoded nucleotides may be added by an unknown mechanism to the 3′ end of linear introns released by the hydrolytic splicing pathway before circularization. The external nucleophilic attack model (*B*) consists of the nucleophilic attack of the 3′-OH residue of a block of non-encoded RNA nucleotides (gray box) at the intron 5′ splice site, ligating it to the intron 5′ end while concurrently displacing exon 1 (step 1). The 3′-OH residue of exon 1 would then attack the 3′ splice site releasing ligated exons and a linear intron harboring non-encoded nucleotides at its 5′ end (step 2). The third transesterification reaction would be initiated by the 2′-OH of the last nucleotide at the 3′ end of the intron (step 3). The position of this final nucleophilic attack would thus dictate how many non-encoded nucleotides are incorporated at the junction of intron circles.

pathway (Fig. 1C), the 3′-OH of free exon 1 would then attack the 3′ splice site releasing ligated exons and a linear intron (step 2). However, in this pathway, the released intron would harbor non-encoded nucleotides at its 5′ end. The third transesterification reaction would then occur within the stretch of non-encoded nucleotides being initiated by the 2′-OH of the last nucleotide at the 3′ end of the intron (step 3). The position of the nucleophilic attack within the exogenous RNA fragment would dictate how many non-encoded nucleotides are incorporated at the intron splice junction.

Even though we cannot completely rule out the incorporation of non-encoded nucleotides through the hydrolytic pathway (Fig. 5A), the presence of relatively long sequences of 27 and 31 nt identical to portions of mRNAs, both in the expected orientation relative to the intron, supports the external nucleophilic attack pathway (Fig. 5B). Interestingly, the release of exon 1 following the nucleophilic attack of cellular RNAs at the 5′ splice junction would stimulate the intron circularization pathway. It would be an alternative to the SER reaction (Fig. 1, SER) to generate free exon 1. Our data also suggest that the perfect intron circles, not harboring extra nucleotides, are generated by the circularization pathway (Fig. 1C). Interestingly, we also detected perfect 5′–3′ intron RNA junctions for a *trans*-splicing variant of Ll.LtrB, fragmented in domain IV just after the LtrA stop codon (S3) (Belhocine et al. 2007). This further suggests that *trans*-splicing introns can also excise through a similar circularization pathway in *L. lactis*. However, the short stretches of non-encoded nucleotides (1–7 nt) present at the splice junction of some circular and alternatively spliced introns are unfortunately too short to identify their origin and confirm their circularization pathway.

The presence of putative intron RNA circles was previously reported for the RmInt1 intron from the bacterium *Sinorhizobium meliloti* (Molina-Sánchez et al. 2006, 2011). RmInt1 seems to share the same circularization pathway as Ll.LtrB as a significant portion of the circular introns released from a maturase mutant also harbors an extra C at the junction (Molina-Sánchez et al. 2006), while removal of the branch point prevents lariat formation and leads to the exclusive release of intron circles also harboring an extra C (Molina-Sánchez et al. 2011). It was recently proposed that the presence of an extra C at the splice junction of in vitro spliced RmInt1 is due to 3′ splice site misrecognition resulting in the inclusion of the first nucleotide of the 3′ exon (Chillón et al. 2014). However, in contrast to Ll.LtrB, long stretches of non-encoded nucleotides were never reported at the splice junction of the putative RmInt1 RNA circles.

Our data also suggest that the circularization pathway for bacterial group II intron is quite different from the circularization of unconventional group II introns from wheat mitochondria. In wheat mitochondria, the presence of stretches of A at the splice junction of intron RNA circles rather suggests that linear introns produced by hydrolysis are circularized following the addition of polyA tails of various length at the 3′ end of the intron (Fig. 5A; Li-Pook-Than and Bonen 2006; Dalby and Bonen 2013). In fact, we did not find any intron splice junction harboring stretches of non-encoded polyAs.

Overall, this study unveils, in addition to intron lariats, the presence of perfect end-to-end intron RNA circles as well as alternatively circularized introns in *L. lactis* RNA extracts for all Ll.LtrB variants studied. This shows that Ll.LtrB does not only excise through the branching pathway in vivo. Taken together, our data shed light on the circularization pathway used by bacterial group II introns in vivo.

MATERIALS AND METHODS

Bacterial strains and plasmids

The *Escherichia coli* DH10β strain was used for both cloning and plasmid amplification, and was grown in LB broth at 37°C with shaking. The *Lactococcus lactis* strain NZ9800Δ*ltrB*::tet (NZ9800Δ*ltrB*) (Tet^R) (Ichiyanagi et al. 2002) was grown in M17 broth supplemented with 0.5% glucose (GM17) at 30°C without shaking. The following antibiotic concentrations were used: chloramphenicol (Cam), 10 µg/mL; spectinomycin (Spc), 300 µg/mL; and kanamycin (Kan), 20 µg/mL.

Some of the plasmids used were previously described in Belhocine et al. (2007): pDL-P_{23}^2-Ll.LtrB-WT (WT), pDL-P_{23}^2-Ll.LtrB-ΔLtrA (ΔLtrA) (amino acids 40–572 in LtrA were replaced by RT [Matsuura et al. 1997]), pDL-P_{23}^2-Ll.LtrB-LtrAMat$^-$ (LtrAMat$^-$) (amino acids SC463 were mutated to LA [Matsuura et al. 1997]),

pLE-P_{23}^2-LtrA. Plasmid pDL-P_{23}^2-Ll.LtrB-ΔA (ΔA) was constructed by site-directed mutagenesis (QuickChange Multi Site-Directed Mutagenesis Kit, Stratagene) (primers in Supplemental Table S2).

Nucleic acids preparations and RT-PCR

Total RNA and nucleic acid were isolated from NZ9800Δ*ltrB* cells harboring different intron variants as previously described (Belhocine et al. 2007). RT-PCR assays were performed as previously described (Belhocine et al. 2007) and the primers used are shown in Supplemental Table S2. Some RT-PCR reaction products (Figs. 3A–C, 4) were labeled with ^{32}P using T4 PNK (New England Biolabs) and ran on 8% PAGE. For Figure 4, 10 µg of total RNA was either untreated, treated with RNase A (Sigma) (30 min), or DNase 1 (New England Biolabs) (2 h) at 37°C before the RT-PCR reactions were performed. For Supplemental Figure S1A, total nucleic acid extract from NZ9800Δ*ltrB*/Ll.LtrB-WT was treated with RNase A as above before PCR followed by cloning in pBS (SmaI). The RNase A treated sample (5 µg) was further digested with BsiWI ON at 55°C before PCR and cloning in pBS (SmaI) (Supplemental Fig. S1B).

Immunoprecipitation of LtrA

Overnight *L. lactis* cultures were diluted (1/25), grown for 7 h and resuspended in 10 mL ice-cold PBS 1×. Formaldehyde was added to a final concentration of 1% and incubated with shaking for 15 min at 25°C. Glycine (20 mM) was added and incubated for an additional 5 min. The cell pellets were washed 2× with 10 mL ice-cold PBS 1× and resuspended in 0.5 mL of lysis buffer (50 mM HEPES–KOH [pH = 7.5], 140 mM NaCl, 1 mM EDTA, 1% Triton X-100, 0.1% sodium deoxycholate, 1 mM PMSF, RNase OUT, proteinase inhibitor 1×); 0.5 mL of cells were mixed with an equal volume of glass beads and vortexed 5× for 30 sec with 1 min intervals on ice. The lysates were cleared by adding $MgCl_2$ (25 mM), $CaCl_2$ (5 mM), RNase OUT, and DNase 1 and incubating the mix for 30 min at 37°C. LtrA polyclonal antibodies (kindly provided by G. Dunny) were added and LtrA was immunoprecipitated ON at 4°C with shaking. Protein A/G conjugated beads and BSA (1 mg/mL) were added and incubated for an additional 4 h. The beads were washed 2× with 0.7 mL of lysis buffer and 2× with 0.7 mL of TE containing 100 mM NaCl. The cross-links were reversed by adding NaCl (200 mM) and proteinase K (20 µg) and incubating 1 h at 42°C followed by 1 h at 65°C. The reactions were centrifuged, the RNAs were recovered from the supernatants (RNeasy Mini Kit, Qiagen) and used to amplify the splice junction of released intron by RT-PCR.

SUPPLEMENTAL MATERIAL

Supplemental material is available for this article.

ACKNOWLEDGMENTS

This work was supported by the National Sciences and Engineering Research Council of Canada (NSERC) under Grant No. 227826 and McGill University. B.C. is a William Dawson Scholar at McGill University.

Received February 19, 2015; accepted March 31, 2015.

REFERENCES

Begel O, Boulay J, Albert B, Dufour E, Sainsard-Chanet A. 1999. Mitochondrial group II introns, cytochrome *c* oxidase, and senescence in *Podospora anserina*. *Mol Cell Biol* **19:** 4093–4100.

Belhocine K, Mak AB, Cousineau B. 2007. *Trans*-splicing of the Ll.LtrB group II intron in *Lactococcus lactis*. *Nucleic Acids Res* **35:** 2257–2268.

Belhocine K, Mak AB, Cousineau B. 2008. *Trans*-splicing versatility of the Ll.LtrB group II intron. *RNA* **14:** 1782–1790.

Carrillo C, Chapdelaine Y, Bonen L. 2001. Variation in sequence and RNA editing within core domains of mitochondrial group II introns among plants. *Mol Gen Genet* **264:** 595–603.

Cech TR. 1986. The generality of self-splicing RNA: relationship to nuclear mRNA splicing. *Cell* **44:** 207–210.

Chee GJ, Takami H. 2011. Alternative splicing by participation of the group II intron ORF in extremely halotolerant and alkaliphilic *Oceanobacillus iheyensis*. *Microbes Environ* **26:** 54–60.

Chillón I, Molina-Sánchez MD, Fedorova O, García-Rodríguez FM, Martínez-Abarca F, Toro N. 2014. In vitro characterization of the splicing efficiency and fidelity of the RmInt1 group II intron as a means of controlling the dispersion of its host mobile element. *RNA* **20:** 2000–2010.

Costa M, Michel F, Toro N. 2006a. Potential for alternative intron–exon pairings in group II intron RmInt1 from *Sinorhizobium meliloti* and its relatives. *RNA* **12:** 338–341.

Costa M, Michel F, Molina-Sánchez MD, Martinez-Abarca F, Toro N. 2006b. An alternative intron–exon pairing scheme implied by unexpected *in vitro* activities of group II intron RmInt1 from *Sinorhizobium meliloti*. *Biochimie* **88:** 711–717.

Cousineau B, Smith D, Lawrence-Cavanagh S, Mueller JE, Yang J, Mills D, Manias D, Dunny G, Lambowitz AM, Belfort M. 1998. Retrohoming of a bacterial group II intron: mobility via complete reverse splicing, independent of homologous DNA recombination. *Cell* **94:** 451–462.

Cousineau B, Lawrence S, Smith D, Belfort M. 2000. Retrotransposition of a bacterial group II intron. *Nature* **404:** 1018–1021.

Dalby SJ, Bonen L. 2013. Impact of low temperature on splicing of atypical group II introns in wheat mitochondria. *Mitochondrion* **13:** 647–655.

Fedorova O, Zingler N. 2007. Group II introns: structure, folding and splicing mechanism. *Biol Chem* **388:** 665–678.

Ferat JL, Michel F. 1993. Group II self-splicing introns in bacteria. *Nature* **364:** 358–361.

Ichiyanagi K, Beauregard A, Lawrence S, Smith D, Cousineau B, Belfort M. 2002. Retrotransposition of the Ll.LtrB group II intron proceeds predominantly via reverse splicing into DNA targets. *Mol Microbiol* **46:** 1259–1272.

Jarrell KA, Peebles CL, Dietrich RC, Romiti SL, Perlman PS. 1988. Group II intron self-splicing. Alternative reaction conditions yield novel products. *J Biol Chem* **263:** 3432–3439.

Lambowitz AM, Zimmerly S. 2004. Mobile group II introns. *Annu Rev Genet* **38:** 1–35.

Lambowitz AM, Zimmerly S. 2011. Group II introns: mobile ribozymes that invade DNA. *Cold Spring Harb Perspect Biol* **3:** a003616.

Li-Pook-Than J, Bonen L. 2006. Multiple physical forms of excised group II intron RNAs in wheat mitochondria. *Nucleic Acids Res* **34:** 2782–2790.

Matsuura M, Saldanha R, Ma H, Wank H, Yang J, Mohr G, Cavanagh S, Dunny GM, Belfort M, Lambowitz AM. 1997. A bacterial group II intron encoding reverse transcriptase, maturase, and DNA endonuclease activities: biochemical demonstration of maturase activity and insertion of new genetic information within the intron. *Genes Dev* **11:** 2910–2924.

McNeil BA, Simon DM, Zimmerly S. 2014. Alternative splicing of a group II intron in a surface layer protein gene in *Clostridium tetani*. *Nucleic Acids Res* **42:** 1959–1969.

Michel F, Ferat JL. 1995. Structure and activities of group II introns. *Annu Rev Biochem* **64:** 435–461.

Molina-Sánchez MD, Martinez-Abarca F, Toro N. 2006. Excision of the *Sinorhizobium meliloti* group II intron RmInt1 as circles *in vivo*. *J Biol Chem* **281:** 28737–28744.

Molina-Sánchez MD, Barrientos-Durán A, Toro N. 2011. Relevance of the branch point adenosine, coordination loop, and 3′ exon binding site for *in vivo* excision of the *Sinorhizobium meliloti* group II intron RmInt1. *J Biol Chem* **286:** 21154–21163.

Murray HL, Mikheeva S, Coljee VW, Turczyk BM, Donahue WF, Bar-Shalom A, Jarrell KA. 2001. Excision of group II introns as circles. *Mol Cell* **8:** 201–211.

Nagy V, Pirakitikulr N, Zhou KI, Chillón I, Luo J, Pyle AM. 2013. Predicted group II intron lineages E and F comprise catalytically active ribozymes. *RNA* **19:** 1266–1278.

Osíewacz HD, Esser K. 1984. The mitochondrial plasmid of *Podospora anserina*: a mobile intron of a mitochondrial gene. *Curr Genet* **8:** 299–305.

Pyle AM. 2010. The tertiary structure of group II introns: implications for biological function and evolution. *Crit Rev Biochem Mol Biol* **45:** 215–232.

Robart AR, Montgomery NK, Smith KL, Zimmerly S. 2004. Principles of 3′ splice site selection and alternative splicing for an unusual group II intron from *Bacillus anthracis*. *RNA* **10:** 854–862.

Schmidt WM, Schweyen RJ, Wolf K, Mueller MW. 1994. Transposable group II introns in fission and budding yeast. Site-specific genomic instabilities and formation of group II IVS plDNAs. *J Mol Biol* **243:** 157–166.

Sharp PA. 1991. Five easy pieces. *Science* **254:** 663.

Stabell FB, Tourasse NJ, Ravnum S, Kolstø AB. 2007. Group II intron in *Bacillus cereus* has an unusual 3′ extension and splices 56 nucleotides downstream of the predicted site. *Nucleic Acids Res* **35:** 1612–1623.

Toor N, Robart AR, Christianson J, Zimmerly S. 2006. Self-splicing of a group IIC intron: 5′ exon recognition and alternative 5′ splicing events implicate the stem–loop motif of a transcriptional terminator. *Nucleic Acids Res* **34:** 6461–6471.

Tourasse NJ, Stabell FB, Reiter L, Kolstø AB. 2005. Unusual group II introns in bacteria of the *Bacillus cereus* group. *J Bacteriol* **18:** 5437–5451.

Vogel J, Börner T. 2002. Lariat formation and a hydrolytic pathway in plant chloroplast group II intron splicing. *EMBO J* **21:** 3794–3803.

Vogel J, Hess WR, Börner T. 1997. Precise branch point mapping and quantification of splicing intermediates. *Nucleic Acids Res* **25:** 2030–2031.